OPEN ACCESS
International Journal of Modern Physics B

© The Author(s)

(2021) 2140052 (16 pages)

DOI: 10.1142/S021797922140052X



Hantavirus outbreaks in the American Southwest: Propagation and retraction of rodent and virus diffusion waves from sky-island refugia

Robert R. Parmenter*,[‡] and Gregory E. Glass^{†,§}

*National Park Service, Valles Caldera National Preserve,
90 Villa Louis Martin, Jemez Springs, NM 87025, USA

†Department of Geography and Emerging Pathogens Institute,
University of Florida, P. O. Box 100009, Gainesville, FL 32610, USA

‡Robert_Parmenter@nps.gov

§qqlass@epi.ufl.edu

Received 1 October 2021 Accepted 10 October 2021 Published 6 November 2021

Hantavirus outbreaks in the American Southwest are hypothesized to be driven by episodic seasonal events of high precipitation, promoting rapid increases in virusreservoir rodent species that then move across the landscape from high quality montane forested habitats (refugia), eventually over-running human residences and increasing disease risk. In this study, the velocities of rodents and virus diffusion wave propagation and retraction were documented and quantified in the sky-islands of northern New Mexico and related to rodent-virus relationships in refugia versus nonrefugia habitats. Deer mouse (Peromyscus maniculatus) refugia populations exhibited higher Sin Nombre Virus (SNV) infection prevalence than nonrefugia populations. The velocity of propagating diffusion waves of Peromyscus from montane to lower grassland habitats was measured at 24.6 ± 5.6 m/day (SE), with wave retraction velocities of 28 ± 8.4 m/day. SNV infection diffusion wave propagation velocity within a deer mouse population averaged 27.5 ± 7.8 m/day, with a faster retraction wave velocity of 161.5 ± 80.7 m/day. A spatiotemporal analysis of human Hantavirus Pulmonary Syndrome (HPS) cases during the initial 1993 epidemic revealed a positive linear relationship between the time during the epidemic and the distance of human cases from the nearest deer mouse refugium, with a landscape diffusion wave velocity of $19.6 \pm 1.0 \text{ m/day}$ ($r^2 = 0.96$). These consistent diffusion propagation wave velocity results support the traveling wave component of the

This is an Open Access article published by World Scientific Publishing Company. It is distributed under the terms of the Creative Commons Attribution 4.0 (CC BY) License which permits use, distribution and reproduction in any medium, provided the original work is properly cited.

[‡]Corresponding author.

HPS outbreak theory and can provide information on space—time constraints for future outbreak forecasts.

Keywords: Climate change; disease; El Niño–Southern Oscillation (ENSO); resource pulse; rodent dispersal.

PACS number: 87.19.Xx

1. Introduction

The scientific understanding of epidemics has improved greatly over the past several decades, through many field and laboratory research projects and with the development of mathematical models of disease dynamics.¹ In particular, zoonotic diseases, involving animal hosts or vectors of disease pathogens (viruses, bacteria and parasites), have received considerable attention by zoologists, ecologists, epidemiologists and mathematicians.^{2,3} Studies on the dynamics and interactions of humans and pathogens using Susceptible, Exposed, Infectious and Recovered (SEIR) populations have been particularly fruitful, especially when details of the ecology of participating species are included.¹ However, many important life-history factors of pathogen, host and vector species remain to be quantified, thereby limiting the accuracy and precision of some zoonotic disease models. Two of these factors are spatial heterogeneity and temporal diffusion of epidemics.

One intensively studied zoonotic disease is the Hantavirus Pulmonary Syndrome (HPS), 4 a respiratory disease in humans caused by rodent-borne viruses in the genus Hantavirus (family Bunyaviridae). HPS provides a useful opportunity to better explore the ecological, epidemiological and mathematical aspects of real-life pathogen-host/reservoir systems. In the United States, numerous species of rodents in the family Muridae are hosts to species-specific serotypes of Hantavirus, having evolved in North America over the past 20 million years. The most serious North American Hantavirus serotype is the $Sin\ Nombre\ Virus\ (SNV)$, 6 carried by the deer mouse ($Peromyscus\ maniculatus$), a common, native widespread rodent species that also frequently inhabits human residences (peri-domestic). Human HPS disease cases are thought to be caused by aerosolized viral transmission from deer mouse urine and feces, inhaled by humans during domestic activities. First discovered during an outbreak in 1993 in New Mexico, Arizona and Colorado, with a mortality rate of 60%, HPS today still has no vaccine or cure, and the mortality rate remains at $\sim 40\%$.

The ecology of SNV and HPS in the western United States has been recently reviewed⁹ and is briefly summarized here. SNV is maintained in populations of deer mice, which typically occupy montane shrubland, woodland and forested habitats at medium to high elevations (> 2100 m).¹⁰ In the Southwest, these habitats occur on "sky-islands", isolated mountainous areas surrounded by lower elevation grasslands and deserts. During periods of increased rainfall (e.g., El Niño events), ecosystem productivity increases with the enhanced growth of plants and insect populations, providing greater food resources for rodents (resource pulse); this, in turn, leads

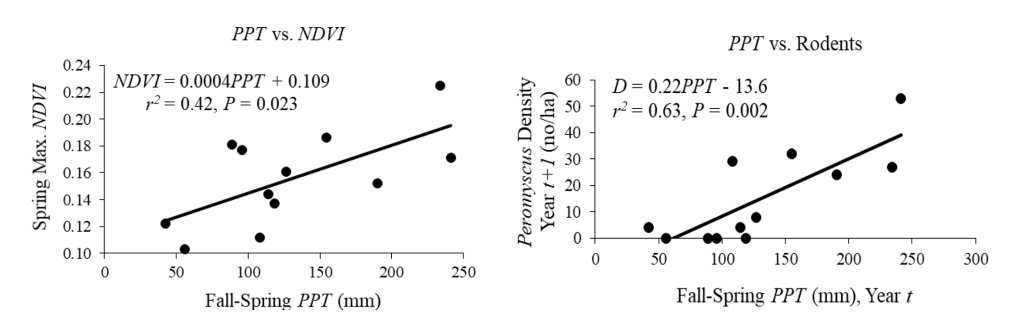


Fig. 1. Left: Relationship between precipitation (PPT) and vegetation production (indexed via the normalized difference vegetation index (NDVI)) on the Sevilleta Long Term Ecological Research site in central New Mexico. Right: Relationship between precipitation and *Peromyscus* density (no/ha) lagged 1 year. Data are adapted from Ref. 5.

to greater rodent reproduction and population density with a time lag of 9–12 months⁹ (Fig. 1). As rodent populations increase, mice disperse in propagating waves into the adjacent grassland/desert habitats that are temporarily suitable due to the additional moisture and food resources. Higher rodent densities also facilitate SNV spread within the deer mouse population. As the propagating wave of deer mice and SNV over-run human residences, rodents enter houses and outbuildings, increasing the human risk of contracting HPS. As the environment returns to normal (drier) conditions, deer mice are unable to survive in the lower-elevation habitats and either return to their mountain refugia or perish in the arid landscape. HPS cases decline as the rodent population retracts or dissolves. An important feature of this conceptual model is that there are high-elevation optimal habitats (termed "refugia") where the deer mouse population always survives under the range of environmental conditions in sufficient densities to maintain the virus population; these refugia serve as the epicenters for periodic diffusive propagating and retracting waves of rodents and virus.¹⁰

Early progress in developing mathematical models of rodents and SNV dynamics incorporated most elements of deer mouse ecology and diffusion waves across a temporally changing landscape. ^{11–13} These models used the Fisher equation to describe the physics of traveling waves,

$$\frac{\partial M}{\partial t} = (b-c)M\left(1 - \frac{M}{(b-c)K}\right) + D\nabla^2 M, \tag{1}$$

where M is the deer mouse population density, b is the birth rate, c is the death rate, K is the habitat carrying capacity and D is the diffusion coefficient.

When a spatial gradient of the habitat heterogeneity function was incorporated, is simulating the elevational change from high-quality refugia to lower-quality habitats, the model shifted to a one-dimensional heterogeneous Fisher–Kolmogorov–Petrovsky–Piskunov equation,

$$\frac{\partial M}{\partial t} = (b - c)M \left(1 - \frac{M}{K(x, t)} \right) + D \frac{\partial^2 M}{\partial t^2},\tag{2}$$

with a space and time-dependent carrying capacity environmental parameter K(x,t) modeling the diversity of habitats.

The basic formulation of the diffusion rate (velocity of the two traveling waves: rodent population spread and the virus infection through the rodent population), ^{11,12} derived from the Fisher equation (Eq. (1)) model above, was

$$v \ge 2\sqrt{D[-b + aK(b - c)]},\tag{3}$$

where v is the velocity and a is the contagion rate between the susceptible and infected mice.

When gradients of habitat types with different carrying capacities were included, ¹⁴ the velocity of the traveling wave was found to be

$$v(\tau) = \sqrt{\frac{rD}{2K(\tau)}}(K(\tau) - 2A(\tau)),\tag{4}$$

where $\tau =$ is the time, r is the intrinsic rate of increase of M, or (b-c), and A is a density-dependent Allee effect parameter.

While the physics and ecological components (functions and parameters) of traveling waves of both the rodent populations across landscapes and virus infection spread within rodent populations have been incorporated into these models, no empirical measures of the velocity (v) of rodent traveling waves propagating from refugia outward to the adjacent sub-optimal habitats have been made in the field. ¹⁴ In addition, the spatial rate of spread of SNV infections within rodent populations during outbreaks remains unknown. Finally, the relationship between landscape-scale diffusion waves of rodents and virus with human populations and HPS disease has not been demonstrated.

Hence, this report (1) summarizes the data from sky-island refugia versus non-refugia habitats with respect to deer mouse SNV infection prevalence, (2) measures the velocity of rodent diffusion wave propagation from sky-island habitats to lower-elevation habitats, (3) documents elevational rates of spread of SNV within a deer mouse population and (4) compares the observed rates of rodent and virus traveling waves with historic landscape-scale patterns of human SNV-caused HPS cases. The results of the field observations were then integrated into the conceptual model to test the model's efficacy in understanding the spatio-temporal dynamics and limits of SNV HPS infections during the outbreak in 1993 in the American Southwest.

2. Methods

2.1. Refugia rodent-virus characterization

To characterize the features of the physical environment that might correspond to refugia for infected mice, locations of human households where the disease had occurred, as well as households without HPS, were geotagged ¹⁵ and monthly 1992–1993 satellite imagery from up to a year prior to the 1993 HPS outbreak were used

to create a spectral signature for HPS risk in a 120,000 km² region.¹⁶ The subsequent five years (1993–1998) were treated similarly and overlain. Areas that were persistently in the highest annual 2.5% tail of HPS risk signature were identified to a 1 ha resolution and the characteristics of elevation, vegetation growth (NDVI) and land cover were measured. These candidate sites for refugia were compared with a random group of sites that were not persistently the highest risk.¹⁰ A further subsample of 40 locations was surveyed for deer mouse populations over two years¹⁷ as described in Sec. 2.2. Changes in local deer mouse population demographics, especially the occurrence of SNV, were compared among three categories of sites: sites that were the highest risk during both the years of monitoring, those that were never in the highest risk and those sites that changed from one year to the next.

2.2. Rodent diffusion wave propagation

Rodent diffusion wave velocities were derived from repeated live-trapping of rodents along a series of transect lines arranged along the length of a large mountain canyon emerging into the grassland in the Cibola National Forest, Sandia Mountains of central New Mexico (Fig. 2, top). Live capture-mark-recapture field sampling of rodents was conducted monthly for three consecutive nights from April 2004 to November 2006; trapping protocols and safety procedures followed the Federal Centers for Disease Control and Prevention (CDC) guidelines. Each transect consisted of ten live-traps at 10-m intervals running perpendicular to the canyon. Wave propagation and retraction velocities (m/day) were calculated using month-to-month changes in distributions among transects, using inter-transect distances and the number of days between sampling periods. Field sampling of rodents was conducted under the University of New Mexico's Institutional Animal Care and Use Committee (IACUC) Protocol #04MCC002 and Animal Welfare Assurance #A4023-01.

2.3. SNV diffusion wave propagation

Propagation waves of SNV infections in rodents were measured over another set of transects in the Redondo Canyon, a high-elevation site in Valles Caldera National Preserve, Jemez Mountains, in northern New Mexico (Fig. 2, bottom). This canyon was inhabited by deer mice along its entire length and had an identified "refugium" near the top of the canyon. Rodents were sampled monthly during the snow-free months (spring through autumn) from 2004 to 2006 using the protocols described above (Sec. 2.2). Blood samples collected from the captured rodents were tested for SNV infection by CDC using the enzyme-linked immunosorbent assay using a SNV recombinant antigen (ELISA). As above, SNV infection wave propagation velocities (m/day) within the deer mouse population were calculated using month-to-month changes in distributions among transects, using inter-transect distances and the number of days between sampling periods.

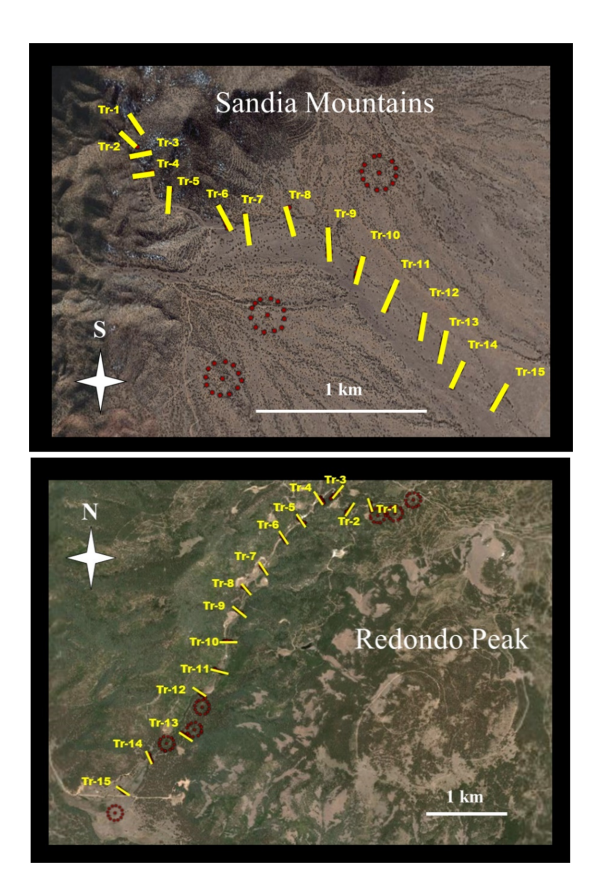


Fig. 2. (Color online) Maps of rodent sampling transects in the (top) Sandia Mountains, Cibola National Forest (2.86 km long, lat. 35°16′ 44″, long. 106°28′ 42″, midpoint elevation 1838 m) and (bottom) Redondo Canyon, Valles Caldera National Preserve, Jemez Mountains, NM (5.68 km long, lat. 35°52′ 50″, long. 106°35′ 15″, midpoint elevation 2615 m). Yellow lines indicate the 100 m trapping transects for dispersal measurements. Red-dot circles are trapping webs for rodent density estimation.

2.4. Diffusion waves and human HPS spatio-temporal patterns

The premise for testing the spatio-temporal patterns of human HPS cases was that if deer mouse populations in montane refugia were expanding outwards from the refugia in traveling waves, with SNV simultaneously propagating through the mouse population, then the prediction would be that human HPS cases closest to the identified refugia would be the first to occur along an outbreak's timeline, and cases later in the outbreak would occur further away from rodent refugia (given the time lags for the rodent diffusion wave to propagate greater distances). As such, the pattern of human HPS cases across the landscape during an outbreak would appear to have a linear positive relationship between time (number of days from the initial HPS case) and the distance from the nearest refugium. The slope of this linear relationship would describe the velocity of wave propagation of the rodents/virus

across the landscape. If the overall wave theory is correct, the predicted outcomes for wave velocities would be that rodent diffusion propagation velocities, virus diffusion velocities, and human HPS wave velocities would all have similar values.

To test this relationship, satellite-derived geographical data on rodent/SNV refugia locations were paired with the nearest locations of residences of human HPS cases from the 1993 outbreak in the Southwest (location and date data were from CDC). A total of 16 residences (of 34 total HPS cases in 1993) were confirmed as highly likely points of human SNV exposure via paired genetic sequencing of local peri-domestic deer mice SNV serotypes and the SNV serotype in the human HPS patients. Measured distances of residences from the nearest deer mouse refugia were then arranged in chronological order from the estimated infection date of the first to last human HPS cases from May to August 1993. Linear regression analysis was used to derive the HPS wave velocity estimate and test for a significant relationship (with P-values representing two-tailed probabilities).

3. Results

3.1. Refugia rodent-virus characterization

The spectral signature associated with where HPS cases occurred during the 1993–1994 outbreak was well defined and most marked at the end of the dry season during

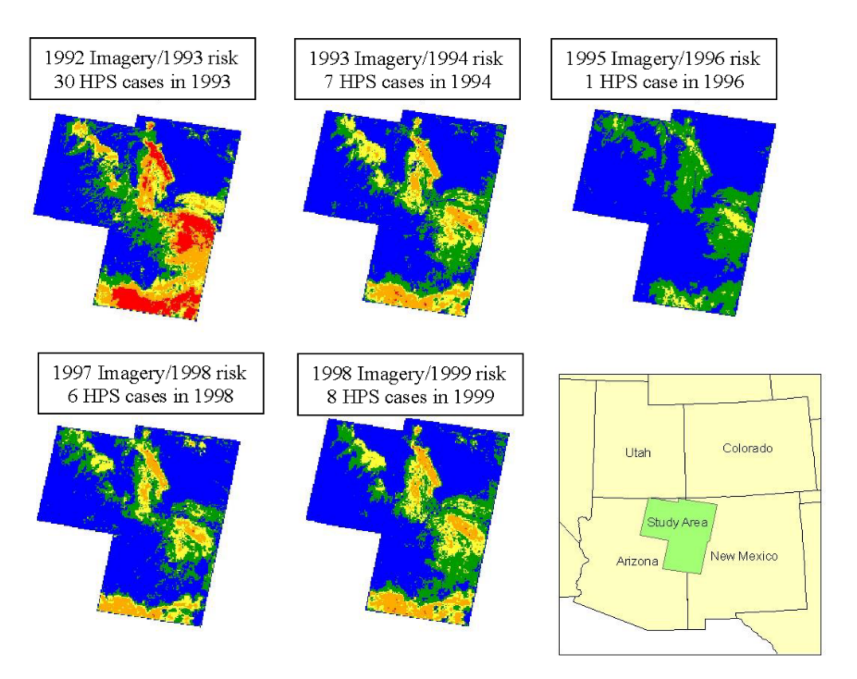


Fig. 3. (Color online) Satellite imagery of areas with high risk of persistent SNV infection prevalence in deer mice (*Peromyscus maniculatus*) populations during 1992–1998, and the number of actual HPS human cases; red colors indicate high SNV prevalence, blue colors indicate low SNV prevalence. Adapted from Ref. 19.

the prior year (June 1992; Fig. 3). The signature was characterized by reflectance in the blue, near- and mid-infra-red portions of the spectrum, as well as higher elevations. The studies showed that, in years in which the environmental signature was not elevated, few human cases occurred (Fig. 3). Examination of multiple years of data showed that a surprisingly small portion of the landscape remained high risk for HPS across multiple years (0.3% of the region). These persistently highest risk sites tended to be on steep slopes above 2100 m elevation and were predominantly, but not exclusively, deciduous or mixed-deciduous/coniferous forests — although not all locations with these land types were persistently high risk. One aspect that distinguished these high risk locations was that they had much longer growing seasons than sites that were not persistently high risk. As such, they were often found in stream valleys and canyons coming from higher elevations. 10

Field data from the identified SNV high risk refugia and low risk sites confirmed that greater proportions of the deer mouse populations were positive for SNV infection in the high risk sites (Fig. 4). Local deer mouse populations in persistently highest risk areas were biased towards the populations that were most likely to carry virus (adult males) and the highest risk areas were the only sites where the deer mouse populations increased during years when overall risk was

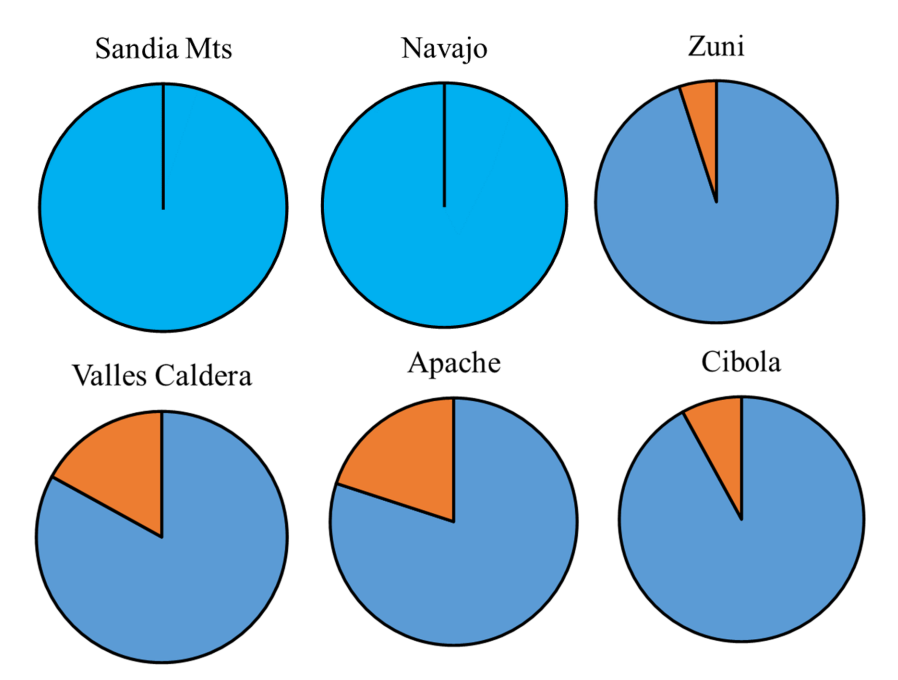


Fig. 4. (Color online) Proportion of deer mice (*Peromyscus maniculatus*) testing positive for SNV (red color) in representative areas identified as low risk (top row) and high risk (bottom row); the total number of sites = 40, data are from 1999. Site risk levels were determined from satellite imagery (see Fig. 3). Mean SNV+prevalences across all sites were 30.8% (n = 185 deer mice) in high risk sites, compared to 8.3% (n = 24) in low risk sites. Data are adapted from Ref. 17.

not elevated. Most importantly, these sites supported populations of SNV-infected mice that persisted from one year to the next.¹⁷ As such, persistently highest risk areas corresponded to proposed conceptual refugia for SNV.

3.2. Rodent diffusion wave propagation

The rodent wave propagation velocities from the Sandia Mountains were calculated from the most abundant species of resident *Peromyscus*, the brush mouse (*P. boylii*). This species is very similar to the deer mouse and carries the *Hantavirus* serotype

Table 1. Dispersal patterns through time of the brush mouse, *Peromyscus boylii*, across trapping transects^a in the Sandia Mountains, NM.

			Sandia Mountains transect number													
	1	2	3	4	5	6	7	8	9	10	11	12	13	14	15	Total
Distance (m)	0	50	50	50	154	250	262	143	251	250	250	231	174	201	269	captures
2004 Apr.	1	5														6
May		8	3	3	1											15
June		5	4	2				1								12
July																0
Aug.			_													0
Sept.		1														1
Oct.		6	2	4									1			13
Nov.		3	6	9	4	3				1				1	1	28
Dec.		5		4	3	2	1	1	1	1	4	1	2			25
2005 Jan.	1	3	2	1	3	2				1						13
Feb.		2	3	1		1	2			2						11
Mar.				2			1				•					3
Apr.	1		2	3												6
May			2			1										3
June		2	2	2	3								1			10
July			1		_											1
Aug.				2												2
Sept.	2	2	1	2			_									7
Oct.	3	2	1	1		2						_				9
Nov.	2	4	5	10		2		2		1	1					27
2006 Jan.	3	4	4	3	1	3		2							1	21
Feb.	4	4	15	5		3										31
Mar.	2	1	3	2		5				1	l					14
Apr.	11	7	14	14	5	2	1		1	3						58
May	5	4	7	1							1					18
June	4	5	3	10	1	1	1			1		•				26
July	1	1		5	2					3						12
Aug.	6	8	5	13	2					2			1	1		38
Oct.	7	8	3	7	7	2				5		2			_	41
Nov.	8	5	1	7	5				3	6	3					38
Total:	61	95	89	113	37	29	6	6	5	27	9	3	5	2	2	489

^aDistances are incremental values between transects from the uppermost transect in the canyon (Transect 1; see site map in Fig. 2). Darkened boxes represent the geographic range of captures. Values are the number of mouse captures on each transect during each sample period.

R. R. Parmenter & G. E. Glass

Table 2. Summary of brush mouse (*Peromyscus boylii*) diffusion wave velocities during rodent wave propagations and retractions from the Sandia Mountains, NM; from data in Table 1.

Wave behavior	Year	Period	Diffusion velocity (m/day)					
Propagation	2004	April–June	15.9					
		September-November	46.1					
	2005	April–June	33.6					
		September-January (2006)	19.3					
	2006	February-May	19.3					
		June-August	13.6					
		Mean:	24.6					
		Standard Error:	5.6					
		95% C.I.:	± 14.5					
Retraction	2004	June-July	32.0					
		November-December	17.4					
		December-January (2005)	17.7					
	2005	February-March	17.3					
		March-April	24.7					
		June-July	76.5					
	2006	January–February	70.0					
		May-June	9.6					
		August-October	9.4					
		October-November	5.5					
		Mean	28.0					
		Standard Error:	8.4					
		95% C.I.:	± 17.6					

Limestone Canyon Virus. Brush mice typically inhabit forests and woodlands at slightly lower elevations than deer mice but also exhibit similar population density dynamics; during high-density periods, brush mice will disperse into the adjacent sub-optimal habitats. A total of 248 brush mice were captured 489 times during the study (Table 1), with 10 of the marked individuals (8 adults and 2 juveniles, and 5 females and 5 males) moving between transect lines during the study; three moved down-slope, six moved up-slope and one moved both up and down. Six periods of population expansion were identified (Table 2). The mean (and SE) diffusion wave propagation velocity was 24.6 ± 5.6 m/day, with a range of 13.6 - 46.1 m/day, while the wave retraction velocity was 28 ± 8.4 m/day (range of 5.5 - 76.5 m/day).

3.3. SNV diffusion wave propagation

In the Redondo Canyon deer mouse population, 222 mice tested positive for SNV out of 1459 mice tested over the three years of the study; males were twice as likely to be SNV⁺ than females, and nearly all age (weight) classes showed infected mice (Fig. 5). Overall, as mouse abundance increased, SNV infection prevalence increased as well, indicating density-dependence (Fig. 6). SNV infection prevalence ranged from 0% to 33.3%, with a mean of 11.1% over the entire study period.

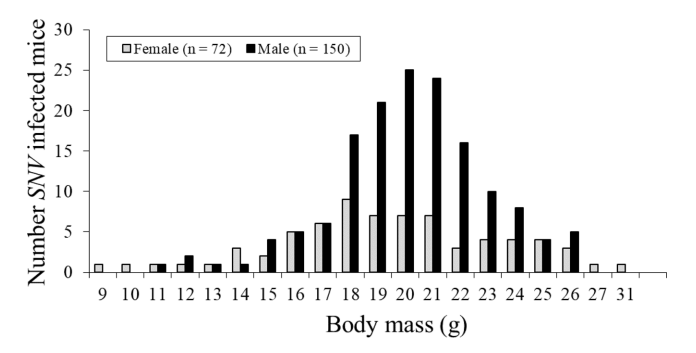


Fig. 5. Demographics of the deer mouse (*Peromyscus maniculatus*) population infected with SNV in Redondo Canyon, NM. A total of 222 mice were positive for SNV out of 1459 deer mice sampled (708 females, 751 males) on all trapping transects and webs. Mean infection rates were 10.2% for females and 20.0% for males.

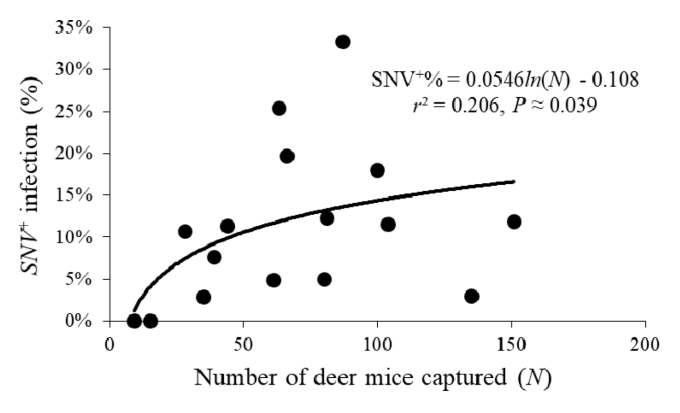


Fig. 6. Relationship between deer mouse (*Peromyscus maniculatus*) abundance and infection prevalence of SNV in Redondo Canyon, NM. Abundance defined as the number of unique mice sampled per three nights of trapping each month on transects. Data are from Table 3.

Propagation of an SNV infection wave within the Redondo Canyon deer mouse population was evident during an SNV outbreak during 2004–2005 (Table 3). In June 2004, SNV⁺ deer mice were only found at high elevations, near the identified refugium location. By the autumn of 2004, SNV⁺ deer mice were found sporadically all along the transects, and during 2005, SNV⁺ deer mice filled in nearly all the transects along the canyon (Table 3). Infection prevalence declined precipitously in 2006, with no SNV⁺ deer mice on the study site in midsummer; some infected mice began reappearing in late summer and fall 2006. Six distribution expansion events were recognized (gray cells in Table 3), producing a mean (SE) virus wave propagation velocity estimate of 27.5 ± 7.8 m/day, with a range of 8.0–59.7 m/day; two SNV⁺ retraction events were observed, with a larger mean velocity value of 161.5 ± 80.7 m/day (Table 4).

Int. J. Mod. Phys. B Downloaded from www.worldscientific.com by 75.161.78.217 on 11/11/21. Re-use and distribution is strictly not permitted, except for Open Access articles.

Numbers of SNV infected deer mice (Peromyscus maniculatus) captured on transects^a during 2004–2006.

Table 3.

	> \ > \	tion		11.4%	11.5%	11.4%	11.5%	3.0%	11.9%	25.4%	33.3%	18.0%	19.7%	12.3%	7.7%	10.7%	0.0%	0.0%	2.9%	5.0%	4.9%	
	NS %	infection		11	11	11	11	3	11	25	33	18	19	12	7	10	0	0	2	ιĊ	4	
	Total	mice		44	104	44	104	135	151	63	87	100	99	81	39	28	6	15	35	80	61	1,098
	Total	SNV+		ഹ	12	ಬ	12	4	18	16	29	18	13	10	3	3	0	0	П	4	33	139
	15	009								-	2		1	2		1				1		6
	14	556								1	2	1	4	1	1							10
	13	902							2	2		1	1									6
	12	415									1			_								1
ıe	11	374									4	2	2									8
qunu	10	451											1									1
Redondo Canyon transect number	6	340								1	1	1			_							3
nyon tı	8	358							2		1	1	1	2								∞
ıdo Ca	7	514									2			1								3
Redor	9	301													_					2		2
	ъ	347								3	9	4	2	1		1						17
	4	254		2	3	2	3		4	4	4	3		2	1							23
	က	300		3	8	3	8	2	2	3	2	3	1		П	1				1	1	31
	2	265								1	3	1							1		1	2
	1	0			Н			1	П		П	1		1							П	7
		Distance (m) 0	Year-Month	2004 June	July	2004 June	July	Sept.	Oct.	2005 June	July	Aug.	Oct.	Nov.	2006 Apr.	May	$_{ m June}$	July	Aug.	Sept.	Oct.	Total

^aDistances are incremental values between transects from the top of the canyon (Transect 1; see site map in Fig. 2). Gray cells show instances of maximum virus spread from the previous month within each year during the outbreak of 2004–2005, upto the peak virus distribution in July 2005, after which SNV+ deer mice began to decline.

Table 4. Summary of SNV diffusion wave velocity rates during virus infection wave propagation and retraction in the Redondo Canyon deer mouse population (*Peromyscus maniculatus*); from data in Table 3.

Wave behavior	Year	Period	Diffusion velocity (m/day)
Propagation	2004	June-July	19.5
		July-September	27.1
		September-October	59.7
	2005	June–July (upslope to Tr 1)	8.0
		June–July (downslope to Tr 7)	23.0
		June–July (downslope to Tr 11)	28.0
		Mean:	27.5
		Standard Error:	7.8
		95% C.I.:	± 19.9
Retraction	2006	May-June	218.5
	2006	September-October	104.4
		Mean:	161.5
		Standard Error:	80.7

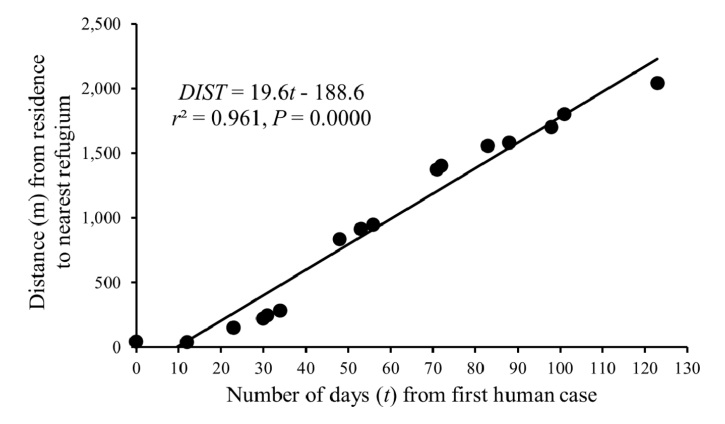


Fig. 7. Spatial-temporal progression of human cases of HPS during the 1993 outbreak in New Mexico and Arizona, USA. Rate of HPS spread from rodent refugia was estimated at 19.6 ± 1.05 m/day. Rodent refugia locations were determined from satellite multispectral data⁹; human HPS case data were from CDC.

3.4. Diffusion waves and human HPS spatio-temporal patterns

The regression of the distance of human HPS case residences from the nearest deer mouse refugium against the timeline of the 1993 HPS outbreak produced a highly significant relationship (Fig. 7).

From May through August, the HPS cases occurred consistently at increasing distances from the nearest refugium, with a maximum distance of ~ 2 km in some of the late August cases. The human HPS case diffusion wave velocity was 19.6 ± 1.05 m/day (SE).

4. Discussion

The results of these studies indicate substantial support for the landscape-level theory of traveling waves of rodents and SNV from sky-island refugia in the American Southwest, propagating outward and over-running human residences, ultimately increasing the risk of human HPS infection. All the observed values of wave diffusion velocities (v in Eq. (4)) proved remarkably consistent: rodent diffusion waves from the Sandia Mountains onto the adjacent grasslands during periods of higher mouse densities averaged 25 m/day; SNV infection diffusion wave velocities in the deer mouse population of the Jemez Mountains averaged 27 m/day; and the observed velocity of human HPS spread across the landscape averaged 20 m/day. The consistency of these values provides increased confidence that the landscape wave theory is supported.

It should be noted that these results can be used to put spatial quantitative constraints on future HPS outbreak forecasts, at least in areas with similar topography. First, by employing year-to-year satellite imagery and multispectral analyses of remote-sensing data, one can identify very specific geographic regions that may be susceptible to HPS outbreaks; such a concept has already been demonstrated prior to the HPS outbreak in 2006, when an increased risk of HPS was forecasted for 2006 based on the 2005 satellite imagery. During 2006, human HPS cases increased to levels of 50% above normal.

In addition, the results herein indicate a geographical limit to the extent of rodent and virus spread across the landscape. In the 1993 HPS outbreak, the disease diffusion wave reached its maximum at 2 km from the known deer mouse refugia, beyond which no additional recorded HPS cases occurred. While future HPS outbreaks will depend on the ecosystem carrying capacities that change through time, and the resulting rodent densities and virus prevalence dynamics, it is extremely unlikely that a wave of HPS cases would cover the entire landscape — deer mouse populations cannot propagate more than a few km from their normal montane refugia habitats. This contributes additional understanding of why HPS appears to be a rural disease, generally not observed in lower-elevation cities and towns (unless residents contract the SNV infection while traveling/visiting in rural areas).

Incorporation of diffusion wave velocity values into models of hantavirus outbreaks should increase the precision and accuracy of predictive models. Inclusion of environmental variables (precipitation, temperature, ecosystem productivity and carrying capacity), rodent population demographics and SEIR dynamics have led to both conceptual and statistical models that are consistent with the observed disease dynamics at landscape scales $^{20-27}$ but have not addressed fine-resolution geographic patterns in rodents, virus and human diseases. With the knowledge of local-scale rates of spread of both reservoir rodent species and hantavirus infections, descriptive models may be developed for higher-resolution understanding and predictions for future disease outbreaks.

Finally, these results have implications for forecasting HPS disease trends with future climate changes. Warming atmospheric temperatures will tend to push species distributions north in latitude and/or higher in elevation. This pattern will tend to shrink deer mouse refugia in woodlands and forests at the higher elevations in southwestern sky-island mountains, with expanding grasslands and deserts moving upward or northward at the expense of forested habitat. Such shifts in habitat types will reduce the areal extent of refugia, and with it the potential area in which rodents and SNV diffusion waves can propagate. Overall, this should theoretically produce a lower risk of human HPS cases at the landscape level; however, increased human habitation of higher-elevation environments (the Wildland-Urban Interface, or WUI) will likely increase the human risk of exposure as residential development expands into rodent and SNV refugia.

Acknowledgments

We sincerely thank our long-term colleague and friend, Professor V.M. (Nitant) Kenkre, for his continued inspiration and counsel in integrating ecology, epidemiology, mathematics and physics over more than two decades of zoonotic disease studies. We also thank the many staff and students who assisted with field data collection. Funding for this research was provided by the National Science Foundation's Ecology and Evolution of Infectious Diseases Program (NSF/NIH EF-0326757), the National Aeronautic and Space Administration (NASA 97CAN01-0048 and NCC5-305), the National Oceanic and Atmospheric Administration (NOAA NA96GP0419), the U.S. National Park Service, the National Centers for Disease Control and Prevention (Dr. Glass performed original data analyses as part of an Inter-governmental Personnel Agreement with the CDC), and the University of New Mexico's Sevilleta Long Term Ecological Research Program (NSF Grants nos. DEB-9411976, DEB-0080529, DEB-0217774, and DEB-0620482). Logistical support was provided by the Sevilleta Research Field Station. This is publication # 940 of the Sevilleta LTER Program. Any use of trade, firm, or product names is for descriptive purposes only and does not imply endorsement by the U.S. Government.

References

- V. M. Kenkre and L. Giuggioli, Theory of the Spread of Epidemics and Movement Ecology of Animals (Cambridge University Press, New York, 2021).
- 2. H. Honarmand, Zoonotic Diseases (1) and (2) (LAP Lambert Publishing Company, Beau Bassin, Mauritius, 2021).
- 3. S. Nandi, Zoonotic Diseases (New India Publishing Agency, Nipa, India, 2020).
- 4. A. MacNeil et al., Virus Res. 162, 138 (2011).
- 5. T. L. Yates et al., BioScience **52**, 989 (2002).
- S. T. Nichol et al., Science 262, 914 (1993).
- 7. J. Toledo et al., J. Infect. Dis. in press, 2021, doi:10.1093/infdis/jiab461.

- 8. R. Perotto, M. L. Fleissner and D. Alfano, Morb. Mortal Wkly. Rep. 34, 45 (2004).
- 9. S. Carver et al., BioScience 65, 651 (2015).
- 10. G. E. Glass et al., Ecol. Appl. 17, 129 (2007).
- 11. G. Abramson et al., Phys. Rev. E 66, 011912 (2002).
- 12. G. Abramson et al., Bull. Math. Biol. 65, 519 (2003).
- 13. G. Abramson et al., Ecol. Complex. 3, 64 (2006).
- 14. G. Abramson et al., J. Theor. Biol. 319, 96 (2013).
- 15. J. E. Childs et al., Am. J. Trop. Med. Hyg. 52, 393 (1995).
- 16. G. E. Glass et al., Emerg. Infect. Dis. 6, 238 (2000).
- 17. G. E. Glass et al., Proc. Natl. Acad. Sci. 99, 16817 (2002).
- 18. J. N. Mills et al., J. Mammal. 76, 716 (1995).
- 19. G. E. Glass *et al.*, *Occasional Papers No. 255* (Museum of Texas Tech University, Lubbock, TX, 2006).
- 20. R. R. Parmenter et al., The Hantavirus epidemic in the Southwest: Rodent population dynamics and the implications for transmission of Hantavirus-associated Adult Respiratory Distress Syndrome (HARDS) in the Four Corners Region, Report to the Federal Centers for Disease Control and Prevention, Atlanta, Georgia. University of New Mexico, Albuquerque, NM, Sevilleta LTER Publication No. 41 (1993).
- 21. H. Tian et al., Proc. Natl. Acad. Sci. 114, 8014 (2017).
- 22. Y. Xiao, Y. H. Zang and M. Gao, Appl. Math. Comput. 360, 28 (2019).
- 23. H. Tian et al., Proc. Natl. Acad. Sci. 115, 4707 (2018).
- 24. V. M. Kenkre et al., Eur. Phys. J. B 55, 461 (2007).
- 25. R. Burger et al., Math. Biosci. Eng. 15, 95 (2018).
- 26. J. L. Liu, Math. Biosci. Eng. 16, 4758 (2019).
- 27. J. L. Liu and T. L. Zang, Nonlinear Anal.-Model. 26, 21 (2021).